Wave Motion 47 (2010) 289–298

Contents lists available at ScienceDirect

Wave Motion

journal homepage: www.elsevier.com/locate/wavemoti

A spectral element solution of the Klein–Gordon equation with high-order treatment of time and non-reflecting boundary

Joseph M. Lindquist *, Beny Neta, Francis X. Giraldo

Department of Applied Mathematics, Naval Postgraduate School, 833 Dyer Road, Monterey, CA 93943, United States

ARTICLE INFO

Article history:
Received 14 May 2009
Received in revised form 5 November 2009
Accepted 24 November 2009
Available online 3 December 2009

Keywords:
Klein–Gordon equation
High-order
Non-reflecting boundary condition
Spectral elements
Higdon
Givoli–Neta
Runge–Kutta

ABSTRACT

A spectral element (SE) implementation of the Givoli–Neta non-reflecting boundary condition (NRBC) is considered for the solution of the Klein–Gordon equation. The infinite domain is truncated via an artificial boundary $\mathcal{B}$, and a high-order NRBC is applied on $\mathcal{B}$. Numerical examples, in various configurations, concerning the propagation of a pressure pulse are used to demonstrate the performance of the SE implementation. Effects of time integration techniques and long term results are discussed. Specifically, we show that in order to achieve the full benefits of high-order accuracy requires balancing all errors involved; this includes the order of accuracy of the spatial discretization method, time-integrators, and boundary conditions.

Published by Elsevier B.V.

1. Introduction

The numerical solution of problems in very large domains has been an active area of research for the last three decades [1]. In the context of fields of application like acoustics, electromagnetics, meteorology, solid geophysics and aerodynamics where dispersive wave problems arise, there are several available methods. The use of non-reflecting boundary conditions (NRBCs) is one such method.

The method of NRBCs can be described as follows. First, the infinite domain is truncated via an artificial boundary $\mathcal{B}$, thus dividing the original domain into a finite computational domain Ω and a residual infinite domain D. Then, a special boundary condition is imposed on $\mathcal{B}$ in order to complete the statement of the problem in Ω (i.e., make the solution in Ω unique) and, most importantly, to ensure that little or no spurious wave reflections occur from $\mathcal{B}$. This boundary condition is called a NRBC, although other names are often used (see [2]). Finally, the problem is solved numerically in Ω, say by the spectral element (SE) method. The SE method is a generalized high-order finite element method where the integration and interpolation points are selected carefully in order to yield accurate but efficient solutions. See Patera [3] and Giraldo–Restelli [4] for more details on this method.

Fig. 1 illustrates the NRBC set-up using an infinite wave-guide. Here, the artificial boundary $\mathcal{B}$ extends from the southern (Γ_S) to the northern (Γ_N) boundaries of the wave-guide, thus creating the east (Γ_E) and west (Γ_W) boundaries of Ω at $x = x_E, x_W$ respectively. Outside of the area enclosed by these boundaries is the residual infinite domain D.

Naturally, the quality of the numerical solution strongly depends on the properties of the NRBC employed. In fact, it can be argued that for many applications (e.g., limited-area atmospheric modeling [4]) the quality of the solution is almost

* Corresponding author. Tel.: +1 831 656 3245.
E-mail addresses: jmlindqu@nps.edu (J.M. Lindquist), bneta@nps.edu (B. Neta), fxgirald@nps.edu (F.X. Giraldo).

0165-2125/$ - see front matter Published by Elsevier B.V.
doi:10.1016/j.wavemoti.2009.11.007

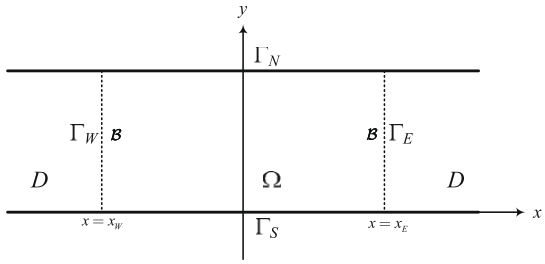

Fig. 1. An infinite channel domain Ω truncated by artificial boundaries Γ_W and Γ_E.

entirely due to the accuracy of the NRBC. In the last 35 years or so, much research has been done to develop NRBCs that, after discretization, lead to a scheme that is stable, accurate, efficient and easy to implement. See [5–8] for recent reviews on the subject. Of course, it is difficult to find a single NRBC which is ideal in all respects and all cases; this is why the quest for better NRBCs and their associated discretization schemes continues.

Recently, *high-order* local NRBCs have been introduced. Sequences of increasing-order NRBCs have been available for a long time (e.g., the Bayliss–Turkel conditions [9] constitute such a sequence), but they had been regarded as impractical beyond 2nd or 3rd order from the implementation point of view. Only since the mid 1990s have practical high-order NRBCs been devised. The present paper is concerned with such a high-order NRBC scheme.

The first *high-order* local NRBC was proposed by Collino [10], for two-dimensional time-dependent waves in rectangular domains. Its construction requires the solution of the one-dimensional wave equation on $\mathcal{B}$. Grote and Keller [11] developed a high-order converging NRBC for the three-dimensional time-dependent wave equation, based on spherical harmonic transformations. Sofronov [12,13] proposed exact boundary conditions for the three- and two-dimensional wave equations in spherical and polar coordinates, respectively (it is proved that NRBCs demonstrated in [11,12] are reduced to each other). Hagstrom and Hariharan [14] constructed high-order NRBCs for the two- and three-dimensional time-dependent wave equations based on the analytic series representation for the outgoing solutions of these equations. For time-dependent waves in a two-dimensional wave-guide, Guddati and Tassoulas [15] devised a high-order NRBC by using rational approximations and recursive continued fractions. Givoli [16] has shown how to derive high-order NRBCs for a general class of wave problems, leading to a symmetric FE formulation. In [17], this methodology was applied to the particular case of time-harmonic waves, using optimally localized Dirichlet-to-Neumann (DtN) NRBCs (see also [18]).

The starting point for the family of NRBCs discussed here is the condition devised by Higdon [19], which was designed for low-order finite difference schemes. Givoli and Neta [20] directly extended the Higdon scheme to high-order finite difference discretizations. They later extended this formulation to one that does not involve any high derivatives (hereafter referred to as the G–N formulation). The elimination of all high-order derivatives is enabled through the introduction of special auxiliary variables on $\mathcal{B}$. This construction demonstrated in [21,22] for finite differences was further extended in [23] for finite element schemes to solve the dispersive wave equation. Hagstrom and Warburton [24] used the Higdon and auxiliary variable framework to develop a symmetric boundary formulation in a full-space configuration where special corner compatibility conditions were developed for the non-dispersive wave equation. Extensions and comparisons between the two methods were published by Givoli and coworkers in [25,26].

In the present paper, the G–N auxiliary formulation of the Higdon NRBC is implemented on a reduced form of the linearized shallow water equations. This formulation has been previously demonstrated in both finite difference and finite element schemes to *arbitrarily high* NRBC order, however, accuracy gains realized by increasing the NRBC order slowed significantly after orders 2 or 3. The formulation used here seeks to remedy this limitation by using a high-order treatment of space (SE) and time (Runge–Kutta) to show the benefits of using a high-order boundary (G–N) scheme. Specifically, the interior and boundary formulations are discretized using high-order basis functions in a stable, equal-order interpolation scheme for all the variables (this does not violate the inf–sup condition). High-order time integration is performed as well in an effort to balance all of the errors involved with the numerical solution. The computational effort associated with the high-order boundary scheme can be shown to grow only *linearly* with the order.

It should be noted that the only other spectral element, high-order boundary approach (to the authors' knowledge) is [27] that is in press. That paper shows similar results for the non-dispersive wave equation on a semi-infinite channel using the Hagstrom–Warburton formulation. The key difference in our work is that we use high-order space, boundary *and* time integration in both a dispersive and non-dispersive wave equation setting.

The following is the outline of the rest of this paper: In Section 2, the problem under investigation is stated. In Section 3, an overview of the G–N auxiliary formulation is presented. In Section 4, a SE semi-discrete formulation is constructed which incorporates a NRBC of this family with any desired order. In Section 5 the time-integrator used to march the equations in time is discussed. The performance of the method is demonstrated in Section 6 via numerical examples.

2. Statement of the problem

As a model serving for introducing the ideas developed here, the shallow water equations are considered. To fix ideas, some specific equations and boundary conditions are chosen here. In the channel (Fig. 1) the 2-D shallow water equations (SWEs) are

$$\begin{aligned}
&\partial_t u + \mu u \partial_x u + \mu v \partial_y u - f v = -g \partial_x \eta,\\
&\partial_t v + \mu u \partial_x v + \mu v \partial_y v + f u = -g \partial_y \eta,\\
&\partial_t \eta + \mu u \partial_x \eta + \mu v \partial_y \eta + (h_0 + \mu \eta)(\partial_x u + \partial_y v) = 0.
\end{aligned} \tag{1}$$

Here t is time, $u(x,y,t)$ and $v(x,y,t)$ are the unknown velocities in the x and y directions, h_0 is the given water layer thickness (in the direction normal to the xy plane), $\eta(x,y,t)$ is the unknown water elevation above h_0, f is the Coriolis parameter, and g is the gravity acceleration. We use the following shorthand for partial derivatives:

$$\partial_a^i = \frac{\partial^i}{\partial a^i}.$$

The parameter μ is 1 for the nonlinear SWEs, and is 0 for the linearized SWEs with vanishing mean flow. We shall consider the latter as a special case in this analysis. It can be shown that this system of equations can be reduced to the dispersive wave equation, also called Klein–Gordon equation (KGE):

$$\partial_t^2 \eta - C_0^2 \nabla^2 \eta + f^2 \eta = S. \tag{2}$$

where $C_0^2 = g h_0$. The goal of this analysis is to solve the analogous homogeneous problem

$$\partial_t^2 u - C_0^2 \nabla^2 u + f^2 u = 0. \tag{3}$$

in the finite domain Ω via SEs. On the south and north channel walls (Γ_S and Γ_N) we have no normal flow, i.e:

$$\frac{\partial u}{\partial y} = 0 \qquad \text{on } \Gamma_N \quad \text{and} \quad \Gamma_S. \tag{4}$$

At $x \to \pm\infty$ the solution is known to be bounded and not to include any incoming waves. To complete the statement of the problem, initial conditions must be given in the entire domain $\Omega \cup D$. To this end, the artificial boundary $\mathcal{B}$ is now introduced at $x = x_E$ and $x = x_W$ to divide between Ω and D as shown in Fig. 1.

3. Auxiliary variables

We present a brief summary of the G–N auxiliary variable process as described in [23]. This auxiliary formulation begins with the Higdon [19] boundary condition given by:

$$H_J: \qquad \left[\prod_{j=1}^{J}\left(\partial_x + \frac{1}{C_j}\partial_t\right)\right] u = 0 \quad \text{on} \quad \Gamma_E. \tag{5}$$

Next, we introduce the auxiliary functions $\phi_1, \ldots, \phi_{J-1}$, which are defined on Γ_E and Γ_W as well as in the exterior domain D (see Fig. 1). Eventually we shall use these functions only on Γ_E and Γ_W, but the derivation requires that they be defined in D as well, or at least in a non-vanishing region adjacent to Γ_E and Γ_W. The functions ϕ_j are defined via the relations

$$\begin{aligned}
&\left(\partial_x + \frac{1}{C_1}\partial_t\right) u = \phi_1,\\
&\left(\partial_x + \frac{1}{C_2}\partial_t\right) \phi_1 = \phi_2,\\
&\vdots\\
&\left(\partial_x + \frac{1}{C_J}\partial_t\right) \phi_{J-1} = 0.
\end{aligned} \tag{6}$$

By definition, these relations hold in D, and also on Γ_E and Γ_W. It is easy to see that (6), when imposed as boundary conditions on Γ_E and Γ_W, are equivalent to the single boundary condition (5). If we also define

$$\phi_0 \equiv u, \quad \phi_J \equiv 0, \tag{7}$$

then we can write (6) concisely as

$$\left(\partial_x + \frac{1}{C_j}\partial_t\right) \phi_{j-1} = \phi_j, \quad j = 1, \ldots, J. \tag{8}$$

This set of conditions involves only first-order derivatives. However, due to the appearance of the x-derivative in (8), one cannot discretize the ϕ_j on the boundary Γ_E alone. Therefore we shall manipulate (8) in order to get rid of the x-derivative.

The function u satisfies the dispersive wave Eq. (3) in D. It is easy to show that the functions ϕ_j satisfy an equation like (3), namely,

$$\partial_x^2\phi_j + \partial_y^2\phi_j - \frac{1}{C_0^2}\partial_t^2\phi_j - \frac{f^2}{C_0^2}\phi_j = 0. \tag{9}$$

Here we need the assumption that C_0 and f do not depend on x or on t.

Givoli et al. [23] have shown that (8), for $j = 1,\ldots,J-1$, is equivalent to

$$\left(\frac{1}{C_j}+\frac{1}{C_{j+1}}\right)\dot{\phi}_j = \phi_{j+1} + \left(\frac{1}{C_j^2}-\frac{1}{C_0^2}\right)\ddot{\phi}_{j-1} + \frac{\partial^2\phi_{j-1}}{\partial y^2} - \frac{f^2}{C_0^2}\phi_{j-1}. \tag{10}$$

As desired, the new boundary condition (10) does not involve x-derivatives. In addition, there are no high y- and t-derivatives in (10) beyond second order.

Rewriting (6), (10) and (7), the new formulation of the Jth-order NRBC on $\mathcal{B}$ can be summarized as follows:

$$\beta_0\dot{u} + \frac{\partial u}{\partial x} = \phi_1, \tag{11}$$

$$\beta_j\dot{\phi}_j - \alpha_j\ddot{\phi}_{j-1} - \phi_{j-1}'' + \lambda\phi_{j-1} = \phi_{j+1} \quad j = 1,\ldots,J-1, \tag{12}$$

$$\alpha_j = \frac{1}{C_j^2} - \frac{1}{C_0^2}, \quad \beta_0 = \frac{1}{C_1}, \quad \beta_j = \frac{1}{C_j}+\frac{1}{C_{j+1}}, \quad \lambda = \frac{f^2}{C_0^2}, \tag{13}$$

$$\phi_0 \equiv u \quad \phi_J \equiv 0. \tag{14}$$

In (12) and elsewhere, a dot indicates time derivative and a prime indicates differentiation with respect to y along $\mathcal{B}$, i.e., the tangential derivative on $\mathcal{B}$.

4. Spectral element method

As a starting point, the semi-infinite channel is considered. This set-up is identical to that described previously, except that at Γ_W, a Dirichlet boundary condition $u(0,y,t) = 0$ is prescribed; see Fig. 2.

Now, the weak form of the problem in Ω is constructed. The solution is sought in the space of trial functions,

$$\mathcal{V} = \{u | u \in H^1(\Omega) \text{ and } u = 0 \text{ on } \Gamma_w\}. \tag{15}$$

Here, $H^1(\Omega)$ is the Sobolev space of square-integrable functions and their first derivatives in Ω. Now, Eq. (3) is multiplied by the basis functions $\Psi_i(x,y) \in \mathcal{V}$ and integrated over Ω so the weak form is (after integration by parts)

$$\int_\Omega \Psi_i u_{tt}\,d\Omega + C_0^2\int_\Omega \nabla\Psi_i\nabla u\,d\Omega - C_0^2\int_\Gamma \Psi_i\vec{n}\cdot\nabla u\,d\Gamma + f^2\int_\Omega \Psi_i u\,d\Omega = 0. \tag{16}$$

Along the eastern boundary, the weak form is found similarly by multiplying (12) by the test function τ_j and integrating it over Γ_E. After integration by parts, simplifying and using (4) to deduce that the boundary term vanishes, this yields:

$$\beta_j\int_{\Gamma_E}\tau_j\dot{\phi}_j\,d\Gamma_E - \alpha_j\int_{\Gamma_E}\tau_j\ddot{\phi}_{j-1}\,d\Gamma_E + \int_{\Gamma_E}\tau_j'\phi_{j-1}'\,d\Gamma_E + \lambda\int_{\Gamma_E}\tau_j\phi_{j-1}\,d\Gamma_E = \int_{\Gamma_E}\tau_j\phi_{j+1}\,d\Gamma_E \tag{17}$$

for $j = 1,\ldots,J-1$, $\phi_j \in H^1(\Gamma_E)$ and any $\tau_j \in H^1(\Gamma_E)$.

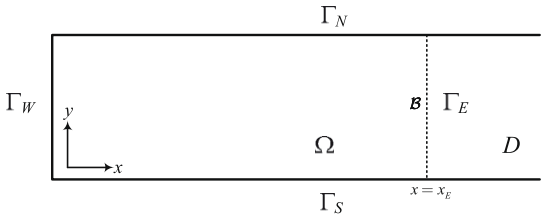

Fig. 2. A semi-infinite channel domain Ω truncated by artificial boundary Γ_E.

Now, utilizing (11) in (16) yields:

$$\int_\Omega \Psi_i \ddot{u}\, d\Omega + C_0^2 \int_\Omega \nabla\Psi_i \nabla u\, d\Omega + f^2 \int_\Omega \Psi_i u\, d\Omega + C_0^2\beta_0 \int_{\Gamma_E} \Psi_i \dot{u}\, d\Gamma_E = C_0^2 \int_{\Gamma_E} \Psi_i \phi_1\, d\Gamma_E. \tag{18}$$

The weak form of the problem is then: find $u \in \mathcal{V}$ and $\phi_j \in H^1(\Gamma_E),\ j = 1,\ldots,J-1$, such that Eqs. (17) and (18) are satisfied $\forall\ \Psi_i \in \mathcal{V}$ and $\tau_j \in H^1(\Gamma_E)$.

Having defined the problem statement we can now introduce the matrix-vector form of the problem. First, in each element, we expand the solution variables u and ϕ_j using the same basis functions used in the weak form as follows:

$$u_N = \sum_{k=1}^{N_p} \Psi_k u^k, \quad \phi_{jN} = \sum_{k=1}^{N_b} \tau_k \phi_j^k, \qquad j = 1,2,\ldots,J-1. \tag{19}$$

Here, N_p refers to the number of points that Ω is discretized into and N_b refers to the number of points that Γ_E is discretized into. Next, we substitute this basis function expansion directly into the weak form (17), (18) and simplify, resulting in the following matrix form of the problem:

$$\begin{aligned} &M\ddot{u} + \beta_0 C_0^2 B\dot{u} + C_0^2 L u + f^2 M u = C_0^2 B\phi_1, \\ &\beta_j M^b \dot{\phi}_j = \alpha_j M^b \ddot{\phi}_{j-1} - L^b \phi_{j-1} - \lambda M^b \phi_{j-1} + M^b \phi_{j+1}, \quad j = 1,\ldots,J-1, \end{aligned} \tag{20}$$

where the matrices $M,\ L,\ B,\ M^b$ and L^b are obtained from analogous element arrays via direct stiffness summation, given by

$$\begin{aligned} &M = \bigwedge_{e=1}^{N_e} M_{ij}^e, \quad L = \bigwedge_{e=1}^{N_e} L_{ij}^e, \quad B = \bigwedge_{e=1}^{N_e} B_{ij}^e, \\ &M^b = \bigwedge_{e=1}^{N_e} M_{ij}^b, \quad L^b = \bigwedge_{e=1}^{N_e} L_{ij}^b. \end{aligned} \tag{21}$$

The expressions for the element arrays are:

$$\begin{aligned} &M_{ij}^e = \int_{\Omega_e} \psi_i \psi_j\, d\Omega_e, \quad L_{ij}^e = \int_{\Omega_e} \nabla\psi_i \nabla\psi_j\, d\Omega_e, \\ &B_{ij}^e = \int_{\Gamma_e} \psi_i v_j\, d\Gamma_e, \quad M_{ij}^b = \int_{\Gamma_e} v_i v_j\, d\Gamma_e, \\ &L_{ij}^b = \int_{\Gamma_e} v_i' v_j'\, d\Gamma_e, \end{aligned} \tag{22}$$

where Ω_e and Γ_e denote, the part of Ω and Γ associated with element e. Also, ψ_i and v_i are the locally defined basis functions from which the global basis functions (Ψ_i and τ_i) are formed. For quadrilateral elements with spectral order N as used in this analysis, ψ_i will be discretized into $(N+1)^2$ points, and v_i into $(N+1)$ points.

For the case of the infinite channel, the set-up is identical, except for the addition of another set of auxiliary variables for use in the western boundary. Since there is no overlap in the contribution of the auxiliary variables to the total solution (i.e. a corner condition) there is no special handling required when solving the dynamic system. The key difference between this work and that presented in [23] are the numerical schemes utilized. This work uses high-order basis functions to discretize the spatial component of this problem with the goal of improving accuracy over linear basis functions. In addition, high-order time-integrators are used in conjunction with the high-order spatial discretization and boundary conditions.

5. Solution of the dynamic system

The system described by (20) and (22) constitute J coupled systems of ODEs that must be solved for $u(x,y,t)$. Our approach uses standard kth order Runge–Kutta (RK) methods to integrate the system in time. Recall that RK is used to solve first order ODEs, and as such, the second order systems described must be converted into a larger system of first order ODEs. Using the substitution $v = \dot{u},\ \dot{v} = \ddot{u}$ and $v_\phi = \dot{\phi},\ \dot{v}_\phi = \ddot{\phi}$ yields the first order systems:

$$\begin{aligned} &\begin{bmatrix} I & 0 \\ 0 & M \end{bmatrix} \begin{bmatrix} \dot{u} \\ \dot{v} \end{bmatrix} = \begin{bmatrix} 0 & I \\ -C_0^2 L - f^2 M & -\beta_0 C_0^2 B \end{bmatrix} \begin{bmatrix} u \\ v \end{bmatrix} + \begin{bmatrix} 0 \\ C_0^2 B\phi_1 \end{bmatrix}, \\ &\begin{bmatrix} I & 0 \\ 0 & \alpha \end{bmatrix} \begin{bmatrix} \dot{\phi} \\ \dot{v}_\phi \end{bmatrix} = \begin{bmatrix} 0 & I \\ -\Lambda & \beta \end{bmatrix} \begin{bmatrix} \phi \\ v_\phi \end{bmatrix} - \begin{bmatrix} 0 \\ u_\Gamma \end{bmatrix}, \end{aligned} \tag{23}$$

where $\phi = \{\phi_1, \phi_2, \ldots, \phi_{J-1}\}^T$, α is the matrix of assembled terms of $\ddot{\phi}$, Λ is the matrix of assembled terms of ϕ, β is the matrix of assembled terms of $\dot{\phi}$ and u_Γ is the vector of terms associated with $\dot{\phi}_1$.

This system was solved using a two-stage approach at each time step. First, the auxiliary system was solved to find the component ϕ_1 required for the main system. Then the main system was solved to find u at the next time step. This process was continued until t_f was reached.

Since this work centers on the use of high-order spectral elements along with high-order boundary conditions, high-order time-integrators were also explored to examine all of the limiting factors of high-order accuracy. We propose that in order to see the full improvements of high-order boundary conditions requires a balance of truncation errors between all of the components of the numerical model; this includes the boundary conditions, the spatial discretization method, and the time-integrators. Experiments were conducted using boundary conditions up to order 10, SE polynomials up to order 16, and time-integrators up to order 10.

6. Numerical experiments

Several numerical experiments were performed to solve both the wave equation ($f = 0$) and the Klein–Gordon equation. In the latter we used $f = 1$. Two different initial conditions were tested. The first is a two-dimensional cosine pulse where b is the height of the channel (in our case we used $b = 3$). For each experiment, Γ_W was introduced at $x_W = -3$. The initial condition is given by

$$u(x, y, 0) = e^{-10x^2} \cos\left(\frac{4\pi y}{b}\right). \tag{24}$$

The other initial condition is a two-dimensional Gaussian centered at $x = 0,\ y = b/2$, given by

$$u(x, y, 0) = e^{-10x^2 - 10(y - \frac{b}{2})^2}. \tag{25}$$

In order to see the effect of the NRBC, we have compared our solution to the same one on a larger domain, i.e. $-3 < x < 9$ for the semi-infinite channel and $-9 < x < 9$ for the infinite channel. Then we solved the problem for time $t = 6.5$ when the disturbance reached the wall at $x = 9$. We consider this reference solution "Exact" when using 8th order basis functions on a 24×8 – element grid (12,545 interpolation points). Time integration was performed with a 4th order Runge–Kutta scheme (RK4) using a time-step chosen to ensure a Courant number of 0.1, where the Courant number is conservatively defined:

$$\text{Courant number} = \frac{C_0 \Delta t}{\sqrt{(\Delta x)^2 + (\Delta y)^2}}. \tag{26}$$

Here, Δx and Δy are chosen as the minimum distance between any two points in the x- or y-directions respectively. This choice is made since the interpolation points are not uniformly distributed when using spectral elements. Additionally, all NRBC parameters C_j were chosen simply as:

$$C_j = C_0 = 1.$$

It should be noted that van Joolen et al. [28] show that this choice of C_j is guaranteed to reduce spurious reflection as the order of the NRBC (J) increases.

In order to quantify the errors observed between the reference and NRBC solutions, we use the normalized L^2_Ω error defined as follows:

$$\|error\|_{L^2_\Omega} = \sqrt{\frac{\sum_{k=1}^{N_p} \left(u_k^{num} - u_k^{ref}\right)^2}{\sum_{k=1}^{N_p} \left(u_k^{ref}\right)^2}}, \tag{27}$$

where N_p is number of points in Ω and u^{num} and u^{ref} are the numerical and reference solutions.

6.1. Semi-infinite channel

For the first experiment, the KGE is examined on a semi-infinite channel with the NRBC at $x_E = 3$. In Fig. 3 we plot the exact solution of the two-dimensional cosine pulse on the top panel and the solution on the truncated domain with NRBC on the bottom panel. The solution on the truncated domain with NRBC uses 4th order basis functions on a 16×8 – element grid using NRBC order $J = 4$. Qualitatively speaking, the results appear to show very little reflection using the combination of high-order basis functions and high order NRBC scheme.

Representative quantitative results can be observed in Fig. 4 showing the error on Ω between the reference and NRBC solutions for increasing NRBC order and various order basis functions. It should be noted that similar results are observed when examining both the wave equation and KGE using either initial condition. Two main points can be extracted from these results.

First, it is clear that increasing the NRBC order yields significant gains in accuracy, but by order 5, the gains observed by lower order basis functions do not continue. This may imply that the error incurred by the interior discretization is more significant than the reflection caused by the NRBC. Second, it is evident that by increasing the order of the basis functions (spectral elements), the gains observed over simply using linear (finite) elements are quite significant. In order to see the gains of a high-order boundary scheme, one must have a high-order interior discretization as well.

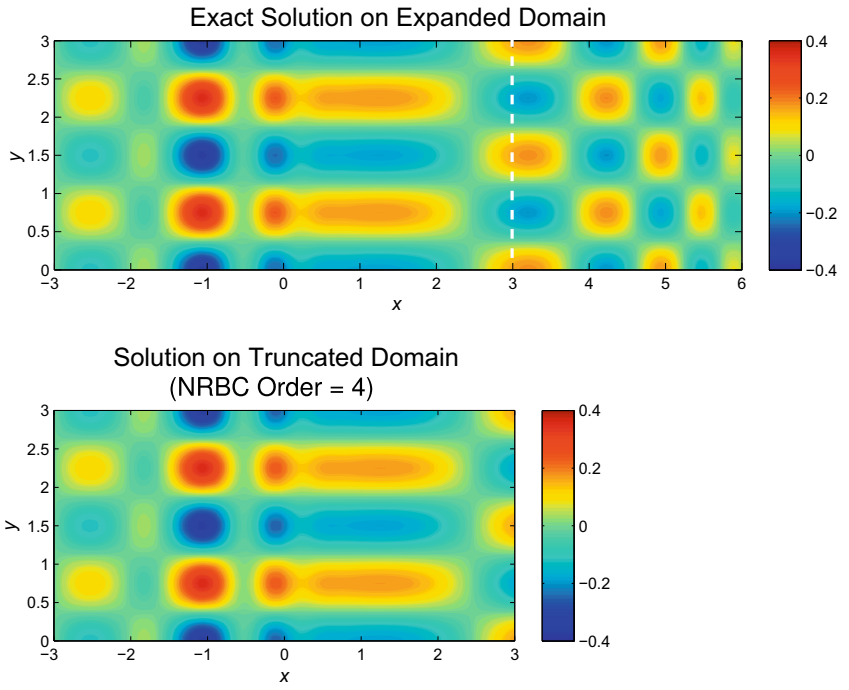

Fig. 3. Dispersive wave guide problem comparing exact and NRBC solutions.

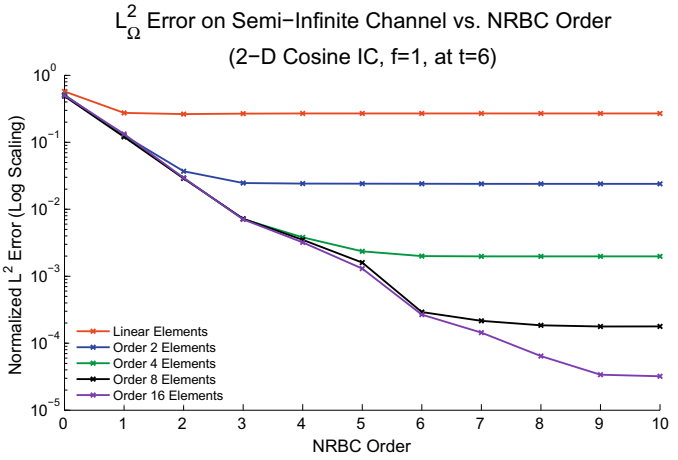

Fig. 4. L^2_Ω error for dispersive cosine pulse IC using various order spectral elements.

6.2. Infinite channel

For the second experiment, the domain is an infinite channel with the NRBCs at $x = \pm 3$. In Fig. 5 we plot the reference solution of the two-dimensional Gaussian on the top panel and the solution on the truncated domain with NRBC on the bottom panel. The solution on the truncated domain with NRBC uses 4th order basis functions on a 16×8 – element grid using NRBC order $J = 4$. Again, qualitatively speaking, the results appear to show very little reflection using the combination of high-order basis functions and high order NRBC scheme.

Representative quantitative results can be observed in Fig. 6 showing the error on Ω between the reference and NRBC solutions for increasing NRBC order and various order basis functions. This plot shows results for the KGE. It should be noted that similar results are observed when examining both the wave equation and KGE using either initial condition. Again, the conclusions are similar to those observed in the semi-infinite channel.

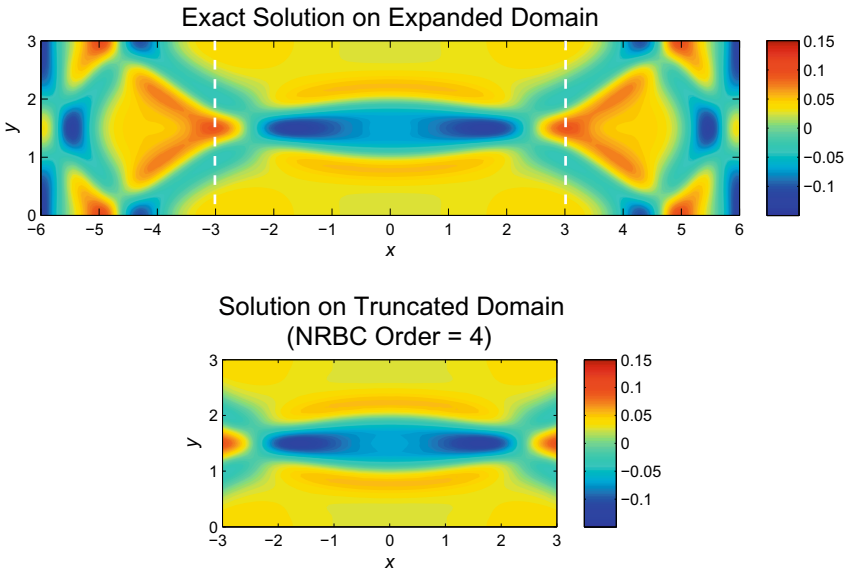

Fig. 5. Dispersive wave guide problem comparing exact and NRBC solutions.

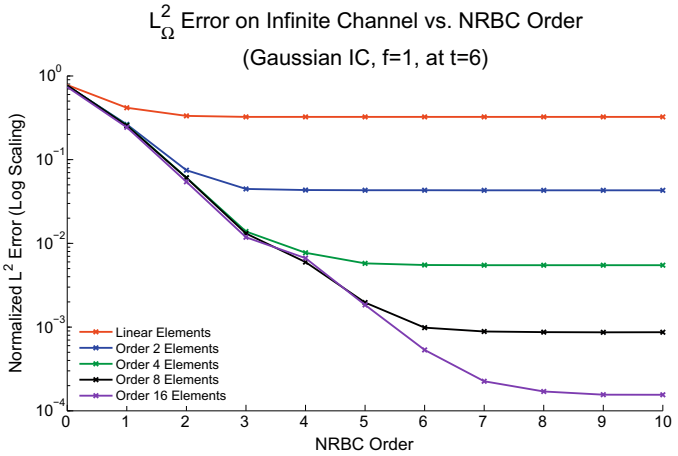

Fig. 6. L^2_Ω error for Gaussian pulse IC using various order spectral elements.

6.3. *Effects of time integration technique*

At the outset of this work, it was believed that at some point the improvements realized by improving the spatial discretization and increasing the order of the NRBC would eventually be limited by the time integration scheme [29]. To this end, the order of the time integration scheme was varied to examine the effects of time integration on accuracy of the solution. As has already been presented, gains made by increasing the order of the NRBC halt for lower order spectral elements after $J = 5$. Even for high-order (orders 8 and 16) spectral elements, the gains made by increasing the order of the NRBC are limited at some point using RK4.

For this experiment, consider the KGE (3) on a semi-infinite domain with $u_{\Gamma_W} = 0$. To ensure that any boundary or time effects are not masked by the interior discretization, 24th order spectral elements are used on a fine mesh consisting of 4753 global points. The Gaussian initial condition is used and is evaluated until $t = 4$. The reference solution in this case was computed as described previously, except this time using 24th order spectral elements on a fine mesh consisting of 9457 global points. Time integration was performed with a 10th order Runge–Kutta scheme (RK10) using a time-step chosen to ensure a Courant number of 0.1.

As can be observed in Fig. 7, gains made by improving the time integration matter only if combined with high-order treatment of the boundary. Conversely – gains using high-order treatment of the boundary can only be realized if there is a high-order treatment of the time integration.

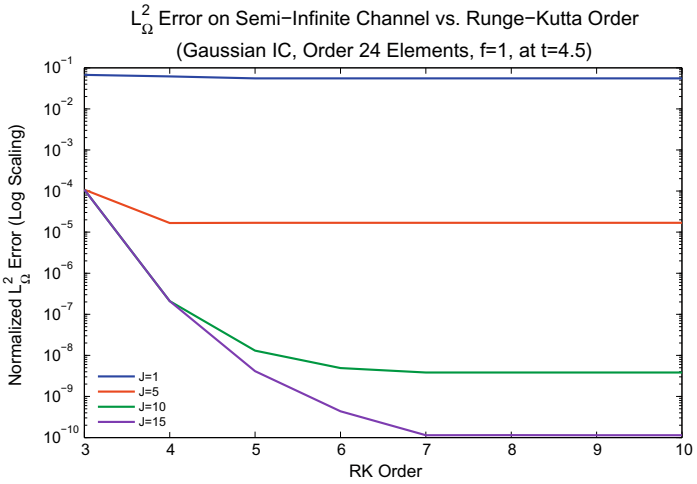

Fig. 7. Error in the SE solution of KGE using NRBCs of various order as a function of time integration order.

It should be noted that these results (error on the order of 10^{-10}) cannot be observed unless high-order treatment of the interior also accompanies the high-order treatment of the boundary and time. Several experiments were conducted which varied the order of the interior, boundary and time integration. The clear result was that without high-order treatment of all components in concert, convergence to the reference solution is stalled.

We believe that results can be improved to machine precision provided all components (interior, boundary and time) have high-order treatment. If high-order treatment of any of the three components is missing, the high-order treatment of the other components is essentially wasted.

6.4. Long term results

In many applications, there is concern for the stability and behavior of the NRBC scheme in the long term. In the final infinite channel experiment, we have run the KGE with $J = 10$ using 8th order basis functions (2145 global points) for $t = 1000$. As can be seen in Fig. 8, by this time the waves have exited the truncated domain and the ripples seen in the figures are of order 10^{-5}. This figure shows that, as expected, in the absence of sources in the domain, the long term result is essentially zero. This would imply long term stability of the method when used in this context.

7. Conclusions

In this paper, we have presented a spectral element solution to the Klein–Gordon dispersive wave equation on a truncated infinite domain in several settings. Using the G–N Higdon-type NRBCs, accuracy was shown to improve significantly in the channel using a combination of high-order (spectral) elements, high-order NRBCs, and (to a slightly lesser extent) high-order time integration techniques. These results suggest a balanced approach to dealing with errors in solving problems of this sort

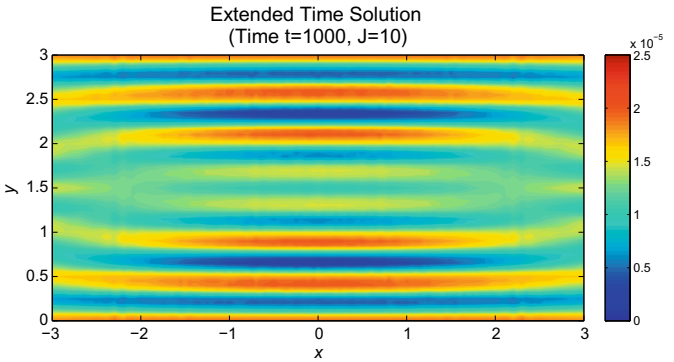

Fig. 8. Extended time ($t = 1000$) KGE solution.

– namely, to make improvements in all major components of the solution (interior, boundary and time discretization) – to see improved accuracy.

Future work includes extending this work to the KGE with non-zero advection and to the full first order SWE system. Further work is also in progress to address quarter and fully open plane problems which are complicated due to the presence of "corners" where two NRBCs intersect. Since the auxiliary variable formulation is itself a system of PDEs, well-posedness requires appropriate boundary conditions – which are not obvious – for each of the auxiliary variables when employed in a "corner-type" configuration. Work is ongoing to further develop the auxiliary variable formulation that will maintain stable, high-order results in the quarter and open domain experiments.

References

[1] D. Givoli, Numerical Methods for Problems in Infinite Domains, Elsevier, Amsterdam, 1992.
[2] D. Givoli, Non-reflecting boundary conditions: a review, J. Comput. Phys. 94 (1991) 1–29.
[3] A.T. Patera, A spectral element method for fluid dynamics – laminar flow in a channel expansion, J. Comput. Phys. 54 (1984) 468–488.
[4] F.X. Giraldo, M. Restelli, A study of spectral element and discontinuous Galerkin methods for the Navier–Stokes equations in nonhydrostatic mesoscale atmospheric modeling: equation sets and test cases, J. Comput. Phys. 227 (2008) 3849–3877.
[5] S.V. Tsynkov, Numerical solution of problems on unbounded domains, a review, Appl. Numer. Math. 27 (1998) 465–532.
[6] D. Givoli, Exact representations on artificial interfaces and applications in mechanics, Appl. Mech. Rev. 52 (1999) 333–349.
[7] T. Hagstrom, Radiation boundary conditions for the numerical simulation of waves, Acta Numer. 8 (1999) 47–106.
[8] D. Givoli, High-order local non-reflecting boundary conditions: a review, Wave Motion 39 (2004) 319–326.
[9] A. Bayliss, E. Turkel, Radiation boundary conditions for wave-like equations, Comm. Pure Appl. Math. 33 (1980) 707–725.
[10] F. Collino, High order absorbing boundary conditions for wave propagation models. Straight line boundary and corner cases, in: R. Kleinman et al. (Eds.), Proc. 2nd Int. Conf. on Mathematical & Numerical Aspects of Wave Propagation, SIAM, Delaware, 1993, pp. 161–171.
[11] M.J. Grote, J.B. Keller, Nonreflecting boundary conditions for time dependent scattering, J. Comput. Phys. 127 (1996) 52–65.
[12] I.L. Sofronov, Conditions for complete transparency on the sphere for the three-dimensional wave equation, Russ. Acad. Sci. Dokl. Math. 46 (1993) 397–401.
[13] I.L. Sofronov, Artificial boundary conditions of absolute transparency for two- and three-dimensional external time-dependent scattering problems, Euro. J. Appl. Math. 9 (1998) 561–588.
[14] T. Hagstrom, S.I. Hariharan, A formulation of asymptotic and exact boundary conditions using local operators, Appl. Numer. Math. 27 (1998) 403–416.
[15] M.N. Guddati, J.L. Tassoulas, Continued-fraction absorbing boundary conditions for the wave equation, J. Comput. Acoust. 8 (2000) 139–156.
[16] D. Givoli, High-order non-reflecting boundary conditions without high-order derivatives, J. Comput. Phys. 170 (2001) 849–870.
[17] D. Givoli, I. Patlashenko, An optimal high-order non-reflecting finite element scheme for wave scattering problems, Int. J. Numer. Methods Eng. 53 (2002) 2389–2411.
[18] D. Givoli, Recent advances in the DtN finite element method for unbounded domains, Arch. Comput. Methods Eng. 6 (1999) 71–116.
[19] R.L. Higdon, Radiation boundary conditions for dispersive waves, SIAM J. Numer. Anal. 31 (1994) 64–100.
[20] D. Givoli, B. Neta, High-order non-reflecting boundary conditions for dispersive waves, Wave Motion 37 (2003) 257–271.
[21] D. Givoli, B. Neta, High-order non-reflecting boundary scheme for time-dependent waves, J. Comput. Phys. 186 (2003) 24–46.
[22] J. Dea, F. Giraldo, B. Neta, High-order, non-reflecting boundary conditions for the linearized 2-D Euler equations: no mean flow case, Wave Motion 46 (2009) 210–220.
[23] D. Givoli, B. Neta, Igor Patlashenko, Finite element solution of exterior time-dependent wave problems with high-order boundary treatment, Int. J. Numer. Methods Eng. 58 (2003) 1955–1983.
[24] T. Hagstrom, T. Warburton, A new auxiliary variable Formulation of high-order local radiation boundary conditions: corner compatibility conditions and extensions to first-order systems, Wave Motion 39 (2004) 327–338.
[25] D. Givoli, T. Hagstrom, I. Patlashenko, Finite element formulation with high-order absorbing boundary conditions for time-dependent waves, Comput. Methods Appl. Mech. Eng. 195 (2006) 3666–3690.
[26] T. Hagstrom, A. Mar-Or, D. Givoli, High-order local absorbing conditions for the wave equation: extensions and improvements, J. Comput. Phys. 227 (2008) 3322–3357.
[27] L. Kucherov, D. Givoli, High-order absorbing boundary conditions incorporated in a spectral element formulation, Commun. Numer. Methods. Eng., in press, doi: 10.1002/cnm.1188.
[28] V. van Joolen, B. Neta, D. Givoli, High-order Higdon-like boundary conditions for exterior transient wave problems, Int. J. Numer. Methods Eng. 63 (2005) 1041–1068.
[29] A.R. Curtis, High-order explicit Runge–Kutta formulae, their uses, and limitations, IMA J. Appl. Math. 16 (1975) 35–53.